

# Isolation and Chemical Characterization of Alzheimer's Disease Paired Helical Filament Cytoskeletons: Differentiation from Amyloid Plaque Core Protein

Alex E. Roher,\* Kenneth C. Palmer,‡ Vincent Chau§ and Melvyn J. Ball||

\*Departments of Anatomy and Cell Biology, ‡Pathology, and §Pharmacology, Wayne State University School of Medicine, Detroit, Michigan 48201; and ||Departments of Pathology, Clinical Neurological Sciences, and Psychiatry, University of Western Ontario, London, Canada N6A 5C1

**Abstract.** The paired helical filaments (PHFs) of Alzheimer's disease were purified by a strategy in which the neurons and amyloid plaque cores of protein (APCP) were initially isolated. This was achieved by several steps of isocratic sucrose centrifugations of increasing molarity and a discontinuous isotonic Percoll density gradient. After collagenase elimination of contaminating blood vessels, lysis of neurons was produced by SDS treatment. The released PHF cytoskeletons were separated from contaminating APCP and lipofuscin by sucrose density gradient. A final step consisted in the chemical purification of highly enriched PHFs and APCP components via a formic acid to guanidine hydrochloride transition. PHFs and APCPs were fractionated by size exclusion HPLC

and further characterized and quantitated by automatic amino acid analysis. We also present some of the morphological and immunochemical characteristics of PHF polypeptides and APCP. Our studies indicate that apart from differences in localization and morphology, PHF and APCP significantly differ in (a) chemical structure (peptide and amino acid composition); (b) epitope specificity (antiubiquitin, antitau, antineurofilament); (c) physicochemical properties (structural conformation in guanidine hydrochloride); and (d) thioflavine T fluorescence emission. These parameters strongly suggest important differences in the composition and, probably, in the etiopathology of PHF and APCP of Alzheimer's disease.

**A**LZHEIMER'S disease (AD)<sup>1</sup> is a primary degenerative dementia characterized by a progressive loss of memory, perception, orientation, reasoning, and judgement that escalates with time until all the intellectual and social functions of the individual are lost (61, 65, 68). Two outstanding histopathological lesions found mainly in the cerebral cortex of the Alzheimer degeneration are the neuritic (senile) plaques and the intracellular neurofibrillary tangles (NFTs) (30, 31, 62, 63). Neuritic plaques are a collection of dystrophic neurites surrounding an extracellular deposition of filamentous structures, known as the amyloid plaque core protein (APCP), whose major component has been recently isolated and characterized (13, 36, 37). Apparently these filaments are produced by the polymerization of a short polypeptide chain (the  $\beta$ -amyloid protein), derived from the pro-

cessing of a much larger precursor (28, 33, 49, 60), which resembles a cell surface receptor and whose mRNA is expressed in neuronal cells (3, 9, 14, 21, 73). The gene responsible for this putative receptor has been mapped to human chromosome 21 (15, 50, 58). However, the cells that ultimately produce these anomalous extracellular amyloid filaments have not been unequivocally identified (36, 42, 52, 62, 63, 67, 69–71). Neurofibrillary tangles represent an intracytoplasmic collection of paired helical filaments (PHFs), made of two helically intertwined 10-nm-diam filaments, with a 70-nm periodicity (30, 31, 62, 63). The origin and precise chemical nature of these filaments are still a highly debated issue (1, 12).

Even though NFTs and neuritic plaques are the major histopathological lesions of AD, they are not restricted only to this disease. Tangles are formed in brains of people with several other neurological disorders including the Parkinson dementia complex of Guam, Down syndrome, and as the result of trauma in the aftermath of boxing (11, 22). Furthermore, tangles and plaques also appear to be components of the brain of normal elderly individuals (64). However, because of the extensive damage that these lesions cause to the central nervous system, tangles and plaques may play an important role in the dementing process of AD.

1. *Abbreviations used in this paper:* AD, Alzheimer's disease; APCP, amyloid plaque core protein; DAB-S, disaggregation buffer containing 10 mM Tris-HCl, pH 7.4, 0.25 M sucrose, 2 mM EDTA, 200 mg/ml PMSF, 500  $\mu$ g leupeptin, 700  $\mu$ g/ml pepstatin, 50 mg/liter Gentamicin sulfate, and 250  $\mu$ g/liter Amphotericin-B; MAP, microtubule-associated protein; NFT, neurofibrillary tangles (light microscopic description); PHF, paired helical filament (electron microscopic appearance); TBS, Tris-buffered saline (10 mM Tris-HCl, pH 7.4, 0.15 M NaCl, and 0.02% Tween-10).

Studies using large pedigrees from a form of familial AD seem to suggest a genetic origin for this type of AD (57). Using restriction fragment length polymorphisms and linkage analysis, the primary genetic defect in these individuals was localized a few centimorgans away from the  $\beta$ -amyloid locus in chromosome 21 (59, 66). This suggests that, while the  $\beta$ -amyloid protein is important for the disease state, it is not the primary defect at least in this form of familial AD. In addition, it has not been shown that either familial AD or sporadic AD (the latter representing the majority of the AD cases) is caused by the same genetic defect.

It has been reported by some investigators that PHFs of AD are chemically identical to the extracellular  $\beta$ -amyloid protein of the neuritic plaque (36). This has become a controversial issue since PHFs seem to carry epitopes shared by normal cytoskeletal components, like the microtubule-associated proteins MAP (34, 47), tau (18, 35, 44, 56, 72), and neurofilaments (2, 10, 39, 41, 47), as well as the proteolytic signal protein ubiquitin (43, 48, 56), all of which apparently are not found in the  $\beta$ -amyloid protein. To compound the issue further, during the isolation process, preparations of PHF tend to be contaminated to a variable degree by filaments from the  $\beta$ -amyloid protein of the neuritic plaque, as well as by other insoluble components (1, 54).

It appears that PHFs substitute for the normal cytoskeletal elements in the affected neurons, mainly microtubules and neurofilaments (16), and affect the shape or form of the cell. Because of their insolubility and increasing accumulation, PHFs become a very important structural component of the cytoarchitecture of AD neurons. Furthermore, even after cellular death these elements remain as neuronal "fossils" or cell "ghosts" (54). Moreover, as mentioned above, PHFs have been shown to carry epitopes of normal cytoskeletal components. For the sake of clarity of definition and to describe more accurately the probable, although anomalous, function of the PHF, we use the term PHF cytoskeletons.

In this paper, we describe a technique for the isolation of neurons from frozen brain tissue. This method eliminates glial cells and blood vessels and leads to the ultimate purification of the pathological PHF cytoskeletons and APCP. In addition, we present biochemical data which indicate that the composition of PHF cytoskeletons differs from those previously published, and more importantly, from the APCP. Following this scheme of purification, PHF cytoskeletons retained epitopes for normal cytoskeletal elements and ubiquitin. Moreover, after depolymerization of PHF cytoskeletons and APCP by formic acid, followed by removal of this denaturing agent, the PHF cytoskeletons failed to reassemble into their native configuration. By contrast, APCP repolymerized into homogeneous 10-nm filaments.

## Materials and Methods

### Isolation of Neuronal Cells

Brains from eight patients who died as the result of AD were obtained within an average period of 8 h postmortem. The right cerebral hemispheres were immediately frozen and stored at  $-70^{\circ}\text{C}$  until the moment of use. The left cerebral hemispheres were histologically processed for diagnostic and morphometric studies. The clinical diagnosis of primary degenerative dementia of Alzheimer type was confirmed in every instance not only by routine neuropathologic examination but also by accepted quantitative criteria. Each case met the diagnostic criteria for neuritic plaques and neurofibrillary tan-

gles recommended by the National Institutes of Health Neuropathology Panel (29). Additionally, each case fulfilled the rigorous morphometric criteria published from the Dementia Study Laboratory, University of Western Ontario (4, 5). A sample of the dramatic histopathologic severity of lesions in these eight hemispheres is provided in Table I. The eight hemispheres used in the present study, were removed from the  $-70^{\circ}\text{C}$  freezer (Revco Inc., West Columbia, SC) and allowed to thaw to  $\sim 15^{\circ}\text{C}$ . Coronal sections (0.5 cm thick) were made and immediately immersed in the disaggregation buffer (DAB-S) at  $4^{\circ}\text{C}$ , containing 10 mM Tris (hydroxymethyl) aminomethane (Tris)-HCl, pH 7.4, 0.25 M sucrose, 2 mM EDTA, 200 mg/liter PMSF, 500  $\mu\text{g}$ /liter leupeptin, 700  $\mu\text{g}$ /liter pepstatin, 50 mg/liter Gentamicin sulfate, and 250  $\mu\text{g}$ /liter Amphotericin B. After dissection of the unwanted white matter, leptomeninges, and large blood vessels from the coronal sections, the cortical grey matter, including hippocampus and amygdaloid nucleus (total yield, 2,000 g) was finely minced with a razor blade, mixed with 6 vol DAB-S and vigorously stirred with a magnetic bar overnight. The tissue suspension was then successively filtered through a series of stainless steel meshes of 1.4 mm, and 700, 300, and 150  $\mu\text{m}$ . The filtered material was centrifuged at 8,000 g for 15 min using a JA-14 rotor (Beckman Instruments, Inc., Palo Alto, CA). The resulting pellets were resuspended in DAB-S to which solid sucrose was added to yield a final sucrose concentration of 0.8 M and centrifuged at 8,000 g for 30 min. The pellets were again resuspended in DAB-S and adjusted to 1.3 M sucrose concentration, filtered through a 150- $\mu\text{m}$  mesh and centrifuged at 15,000 g for 30 min. The dense layer floating at the top of the centrifuge bottles was vacuum aspirated. The pellets at the bottom of the bottles were resuspended in DAB-S at a final concentration of 1.9 M sucrose and centrifuged at 50,000 g for 30 min using an SW-28 rotor (Beckman Instruments, Inc.). The compact top layer was removed with a spatula. This material was resuspended in DAB-S, in which the 0.25 M sucrose was substituted by 0.15 M NaCl (DAB-NaCl), and submitted to a discontinuous NaCl-isotonic Percoll (Percoll 400) density gradient centrifugation (700 g for 30 min, at  $20^{\circ}\text{C}$ ). The gradient was formed by 10 ml each of 44, 34, 27, and 20% Percoll concentrations. The fractions contained at the 44/34, 34/27, and 27/20% interfaces were washed four times with 50 mM Tris-HCl, pH 8.0, 2 mM  $\text{CaCl}_2$  at 1,500 g for 10 min, resuspended in the same buffer to which 0.2 mg/ml of collagenase (CLS III; Worthington Biochemical Corp., Freehold, NJ) and 10  $\mu\text{g}$ /ml of DNase I (Calbiochem-Behring Corp., San Diego, CA) were added, and incubated at  $37^{\circ}\text{C}$  for 14 h. Removal of enzymes and their byproducts and recovery of neurons was achieved by repetitive washes (1,500 g, 15 min) with 0.15 M NaCl.

### Preparation and Purification of Paired Helical Filaments

Neurons were resuspended in 4 vol of 0.15 M NaCl followed by the addition of 15 vol of 2% SDS, 50 mM Tris-HCl, pH 8.0. Cellular lysis was allowed to proceed for 30 min at room temperature with intermittent gentle shaking. All soluble cellular components were removed by centrifugation at 1,500 g for 30 min. The brown pellets were washed twice more with 1.5% SDS under the same conditions. The recovered pellets (from the initial

Table I. Morphometric Features Confirming Diagnosis of Alzheimer's Disease

Age	Sex	Morphometric observations* (hippocampal cortex)		
		Adjusted tangle index/ $\text{mm}^3$	Adjusted granulovacuolar index/ $\text{mm}^3$	Neuronal density/ $\text{mm}^3$
63	F	159.8	317.1	3,500
78	M	27.9	403.4	3,898
74	M	168.1	452.1	5,857 $\ddagger$
77	F	93.3	292.1	2,548
76	M	136.1	426	5,551
84	M	80.2	251	5,185
69	M	113.6	223.5	3,806
74	M	101.8	322.1	4,995

\* Of these 24 parameters quantified in the eight cases, 23 exceed the minimum severity required (tangles  $>20/\text{mm}^3$ ; granulovacuoles  $>55/\text{mm}^3$ ; neurons  $<5,600/\text{mm}^3$ ).

$\ddagger$  In one case, two of the three lesions exceed the minimum, but only one of three need do so to confirm the diagnosis (4).

2,000 g of gray matter) contained PHF cytoskeletons, ACP, lipofuscin granules, and a small amount of unidentified insoluble cell debris. These pellets were resuspended in 50 ml of 1.5% SDS and submitted to a discontinuous sucrose density gradient prepared in 50 mM Tris-HCl, pH 8.0, 1.5% SDS and formed by 2 ml each of 2.1, 2.0, 1.7, 1.4 M sucrose and 1.5 ml each of 1.3 and 1.2 M sucrose, respectively. A total of 48 gradient tubes (14 × 89 mm) were prepared. A 1-ml aliquot of the above SDS-insoluble material was loaded at the top of each of the tubes and centrifuged at 200,000 g for 1 h at 20°C in an SW 41 Ti rotor (Beckman Instruments, Inc.). The resulting interfaces were aspirated with a peristaltic pump and the sucrose removed by dilution and three washes with 0.5% SDS in 25 mM Tris-HCl, pH 8.0. The 2.1/2.0-M interface contained more than 90% pure PHF cytoskeletons; the remaining 10% consisted of lipofuscin granules and a negligible amount of ACP. The 2.0/1.7-M interface was composed of 80% PHF cytoskeletons. The 1.7/1.4-M interface, on the other hand, contained 80% ACP, 20% PHF cytoskeletons (of smaller size and sparser concentration) and lipofuscin granules. The 1.3/1.4-M interface was composed of ACP and lipofuscin.

Since the largest quantity of PHF cytoskeletons localized at the 2.0/1.7-M sucrose interface, we further enriched these structures by resuspending them in 1.0 M sucrose, 0.5% SDS, followed by centrifugation at 200 g for 15 min in conical 1.5-ml reactive vials. A small brown pellet, mainly lipofuscin plus some PHF cytoskeletons and some large ACP aggregates, collected at the bottom of the vial. The supernatant was recentrifuged at 600 g for 15 min, yielding a small brown pellet. The pellet was discarded and a large pale brown intermediate layer plus a whitish turbid supernatant were subsequently recovered by centrifugation at 1,500 g. These latter two fractions contain more than 95% PHF cytoskeletons, which differed only in their sizes and degree of filament aggregation.

Further purification of the PHF proteins was obtained by dissolving a pellet of 150 µl of PHF cytoskeletons in 2.2 ml of concentrated (89%) formic acid, allowed to stand at room temperature for 20 min, followed by centrifugation at 1,500 g for 10 min. The supernatant was collected and centrifuged at 12,000 g for a further 10 min. The two centrifugations permitted the elimination of a small amount of remaining lipofuscin granules, mainly those entrapped in the network of PHF cytoskeletons. The supernatant containing the solubilized PHF proteins was then dialyzed (dialysis tubing cut off 1,000 D) against two changes (500 ml each) of 6 M guanidine-hydrochloride (GHCl), 125 mM Tris-HCl, pH 8.0, 5 mM DTT. When the first dialysis buffer reached a pH of 4.0 (~4 h), the dialysis bag was transferred to the second vessel whose pH, overnight, equilibrated at 7.5. The clear content of the dialysis bag was then centrifuged in polyallomer tubes at 250,000 g for 20 min (TLA 100.2 rotor; Beckman Instruments, Inc.). A minute pellet, estimated to be no more than 2 µl, was produced. The clear supernatant was stored at -70°C until the moment of use.

### Purification of ACP

The materials collected at the 1.7/1.4- and 1.4/1.3-M sucrose gradient centrifugation described above were enriched with ACP. To remove the contaminating lipofuscin, a sucrose-free aliquot of 900 µl, pooled from both interfaces, was washed three times with 15 ml of distilled water (1,500 g, 10 min). The resulting pellet was then thoroughly resuspended in 6 ml of 89% formic acid and, after standing at room temperature for 20 min, centrifuged at 1,500 g for 15 min. Most of the lipofuscin granules were collected at the bottom of the tube. The pale yellow supernatant was centrifuged once again at 12,500 g for 10 min. The resulting clear supernatant was dialyzed against 6 M GHCl in the same manner as described for the purification of PHF protein but excluding the DTT. When the pH of the dialysis buffer reached 3.0, a white flocculent precipitate formed in the bag. After a second change of the dialysis buffer (pH 7.5), the precipitated material was recovered by centrifugation at 12,500 g for 10 min. The pellet, which had a semitransparent jellylike consistency, contained the repolymerized 10-nm filaments of the ACP. This material was washed twice with dialysis buffer and stored at 4°C.

### Morphological Analysis

All experimental steps involved in neuronal isolation, preparation of PHF cytoskeletons, and ACP purification were monitored by phase and fluorescence microscopy, as well as by transmission electron microscopy. A rapid technique which permitted the detailed analysis of neuronal integrity was achieved by staining the cells with either the carbocyanine D272 (3,3'-dipentylloxocarbocyanine iodide) or the carbocyanine D378 (3,3'-diheptyloxocarbocyanine iodide) obtained from Molecular Probes, Inc. (Junction City,

OR). An aliquot of the cell suspension to be morphologically assessed was washed with 0.15 M NaCl, 10 mM Tris-HCl, pH 7.4 and resuspended in 10 vol of the same buffer. 10 µl of cell suspension was spread on a slide, allowed to dry in an oven at 37°C for 15 min and fixed in absolute ethanol for 15 min. After rinsing with distilled water, the slides were stained for 2-3 min with a 25-µg/ml solution of carbocyanine (stock solution, 1 mg/ml ethanol), prepared in 10 mM Tris-HCl, pH 7.4, and, just before use, acidified with HCl to a concentration of 0.05%. The slides were then rinsed in distilled water, mounted in Bacto FA fluid (Difco Laboratories Inc., Detroit, MI) and observed in an Axiophot epifluorescence microscope (Carl Zeiss, Inc., Thornwood, NY), equipped with an excitation filter (450-490 nm) and a barrier filter (520 nm).

The presence of PHF cytoskeletons and ACP was monitored by thioflavine T staining. We chose this fluorochrome because under acidic conditions it permitted a clear distinction between these two filamentous structures. When excited at 350 nm, PHF cytoskeletons stained bright green and ACP a silver or deep blue. A drop of the specimen to be assessed was spread on a slide, air dried, and fixed in absolute ethanol for 1 h. Thioflavine T (250 mg) was dissolved in 5 ml of absolute ethanol, and the volume made up to 50 ml with 50 mM Tris-HCl, pH 8.0. To acidify the solution, 400 µl of concentrated HCl was added before use. The fixed specimens were rinsed with water and stained for 10 min. After rinsing away the excess fluorochrome with water, the slides were mounted using Bacto FA fluid (Difco Laboratories, Inc.) and observed in a fluorescence microscope (excitation filter, 370 nm). When necessary, the quantity and quality of the purified PHF cytoskeletons and ACP preparations were determined by transmission electron microscopy, using Formvar-coated grids stained for 4 min with 1% aqueous uranyl acetate and observed on a 100 CX microscope (JEOL USA, Electron Optics Div., Peabody, MA) at 60 kV.

### Light Microscopic Immunocytochemistry

**Purity of Neuronal Preparation.** Determination of the glial contamination in our neuronal preparations was made by immunocytochemistry using a monoclonal antibody against galactocerebroside and polyclonal antibodies against myelin basic protein and glial fibrillary acidic protein. A cell suspension (100 µl) was washed with 10 mM PBS (Na<sub>2</sub>HPO<sub>4</sub>, pH 7.2, 0.15 M NaCl) and resuspended in 100 µl of 4% paraformaldehyde. After 15 min at room temperature the cells were washed three times with PBS and incubated with 200 µl of either normal mouse or rabbit serum (1:20 dilution) containing 3% BSA. This was followed by three washes with PBS and the addition of the above-mentioned antibodies diluted 1:50 in PBS. After a 1-h incubation, the specimens were washed three times with PBS, 200 µl of FITC-labeled goat anti-mouse or goat anti-rabbit serum (1:100 dilution) was added accordingly, incubated 45 min at room temperature, washed three times with PBS, and mounted with a drop of Bacto FA fluid (Difco Laboratories, Inc.).

**PHF Preparations.** Diluted aliquots of PHF cytoskeletons recovered from the final centrifugation steps were spread on clean glass slides and dried at 37°C for 1 h. The slides were washed twice with PBS and incubated with normal goat serum (diluted 1:5 with PBS) for 5 min. After three 15-min washes with PBS, the slides were incubated with primary antibody (1:100 for antiubiquitin and antitau; 1:50 for antineurofilament) for 30 min at room temperature. Slides were again washed three times with PBS and incubated with the second antibody conjugated to FITC (goat anti-rabbit IgG for ubiquitin and tau or goat anti-mouse IgG for neurofilament protein—all diluted 1:50) for 30 min at room temperature. After incubation, the slides received three washes with buffer, gently blotted and mounted in Bacto FA medium (Difco Laboratories, Inc.) for fluorescence microscopy. In an additional series of experiments, PHF preparations were double stained with rhodamine- and fluorescein-labeled second antibody (TRITC-goat anti-rabbit IgG against tau and FITC-goat anti-mouse IgG against neurofilament) using the same protocol as above.

### Immunostaining of PHF Proteins

Immunoreactivity of PHF proteins was assessed by immunostaining on a dot blot as follows: 2-µl aliquots of the proteins to be investigated were spotted directly onto nitrocellulose filters (BA85; Schleicher & Schuell, Inc., Keene, NH) and washed twice with 20 ml of Tris-buffered saline (10 mM Tris-HCl, pH 7.4, containing 0.15 M NaCl and 0.02% Tween-10; TBS) to remove any residual GHCl. The filters were then blocked with a solution containing 2% ovalbumin in TBS for 1 h. Proteins bound on the filters were assayed for their immunoreactivity to antibodies directed against ubiquitin, tau, and neurofilament proteins with secondary antibodies conjugated with

alkaline phosphatase (7). Antibodies directed against ubiquitin were raised in rabbits with ubiquitin conjugated to keyhole limpet hemocyanin (20), as has been described by Meyer et al. (38). Antibody against tau was obtained from ICN Biomedicals, Inc. (Costa Mesa, CA) and that against neurofilament (8D8) was a generous gift from Dr. Brian Anderton, St. George's Hospital, London, England.

### Amino Acid Analysis

Amino acid analysis of proteins was carried out in 6 M HCl, containing 1.0% phenol, in melting point tubes at 108°C for 24, 48, and 72 h. Alternatively, hydrolysis was performed at 150°C for 75 min on a PicoTag workstation (Waters Instruments, Inc., Rochester, MN). After removal of the acid in a *spædvac* centrifuge, the specimens were derivatized to form phenylthiocarbonyl amino acids and separated by HPLC on a Novapack C18 column (Waters PicoTag; Waters Instruments, Inc.).

### HPLC

300- $\mu$ l aliquots of the PHF peptides, soluble in 6 M GHCl, were centrifuged at 250,000 g for 20 min (TL 100.2 rotor, Beckman Instruments, Inc., Palo Alto, CA) and submitted to size exclusion chromatography on a TSK 3000 SW column (600  $\times$  7.5 mm; Beckman Instruments, Inc., Altex Division, San Ramon, CA) with a mobile phase of 6 M GHCl containing 5% formic acid.

The material precipitating in 6 M GHCl, containing the APCP peptides, was separated from the soluble PHF in the supernatant by centrifugation. The resulting pellet was twice washed with 6 M GHCl, resolubilized by the addition of 8 vol of 88% formic acid and dialyzed (membrane cut off of 1,000 D) against four changes (500 ml each) of 70% formic acid for 4 h at 2°C. The optically transparent specimen was centrifuged at 250,000 g for 20 min at 4°C. Aliquots of 300  $\mu$ l were chromatographed on a Superose 12 size exclusion column (300  $\times$  10 mm; Pharmacia Fine Chemicals, Piscataway, NJ) using as mobile phase 70% formic acid.

### Results

The purification scheme used in the present investigation is succinctly summarized in Fig. 1. We found that, in spite of having remained frozen at -70°C for an average period of 60 mo, the AD brain tissue used in this study yielded neurons which, morphologically, did not differ from those isolated in our laboratory from fresh tissue processed immediately postmortem. We believe that an important step in the conservation of cell morphology was the sectioning and initial processing of the brain cortex in isotonic sucrose while still frozen. In addition, the incorporation of enzyme inhibitors in the freshly made disaggregation buffers helped to prevent undesirable proteolysis of cells. Gentle filtration of the brain tissue through a series of decreasing aperture stainless steel meshes, instead of the use of nozzle aspiration or syringe pressure forcing, minimized the unavoidable mechanical trauma to the cells. An example of the quality of preservation of the neurons obtained up to this point is illustrated in Fig. 2. A series of preliminary studies established that the best routine for the enrichment of the cellular population consisted of the bulk elimination of myelin and cell debris, derived from the mincing of the tissue and subsequent filtration, by centrifugation in 0.8 M sucrose. These materials floated at the surface of the centrifuge bottle or loosely accumulated at the surface of the bottom pellet and were eliminated by careful and fast decantation. Increasing the sucrose concentration to 1.3 M, followed by centrifugation, resulted in the formation of a large aggregation of material at the top of the bottle. Because of its compact consistency, this material was removed by vacuum aspiration. Microscopic examination showed it to consist of glial cells, blood vessels, cell processes, and other cell debris. When the sucrose concen-

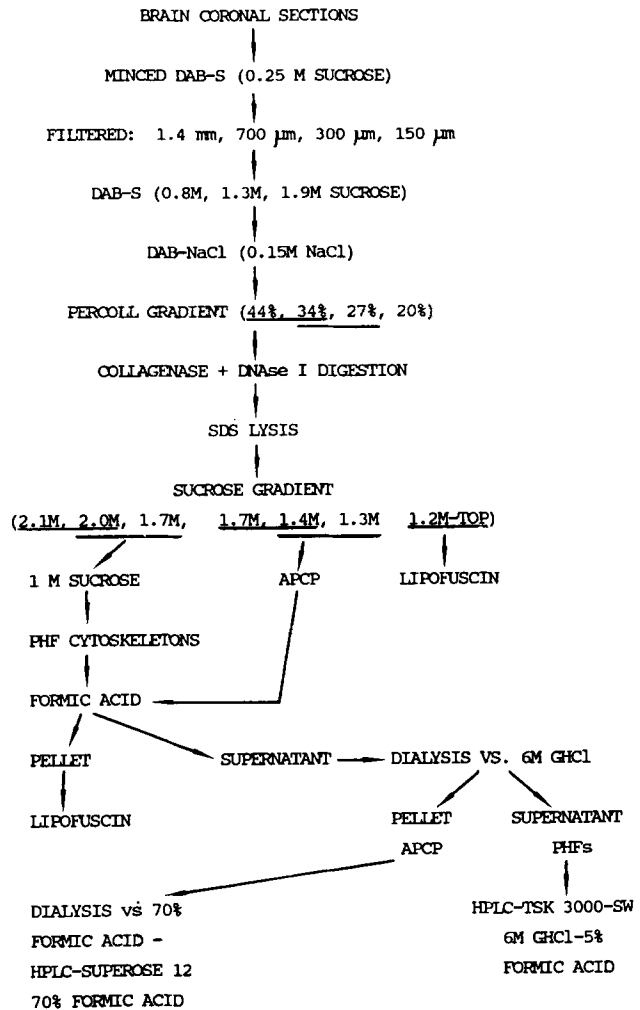


**Figure 1.** A flow chart summarizing the strategy used in our laboratory for the purification of PHFs and APCP of AD. This consisted of (a) isolation of neurons and amyloid cores, (b) lysis of cells by SDS, (c) separation of PHF cytoskeletons, APCP, and lipofuscin via a sucrose gradient, and (d) a final physicochemical purification of PHF and APC polypeptides.

tration was increased to 1.9 M, the enriched neuronal population floated on the surface of the medium as a semisolid pellet that was easily scooped out with a spatula, whereas the pellet at the bottom of the tube contained numerous free nuclei. Percoll density gradient centrifugation further enriched the neuronal fraction.

The use of antibodies against the oligodendrocyte antigens (myelin basic protein and galactocerebroside) and against the astroglial marker (glial fibrillary acidic protein) revealed the presence of two glial cells per 3,000 neurons in the 44/34% Percoll interface. The 34/27 and 27/20% Percoll interfaces contained 2 and 10% glial cells, respectively. The materials retained at the top of the gradient (20% Percoll and above) and at the bottom of the tube were discarded. However, small blood vessel fragments of various sizes still contaminated the enriched neuronal interfaces. Since our objective was to further concentrate the neuronal population containing the PHFs of AD, we decided to use collagenase. This enzyme completely eliminated the remaining blood vessels. Unfortunately, a number of the neuronal processes were detached from their

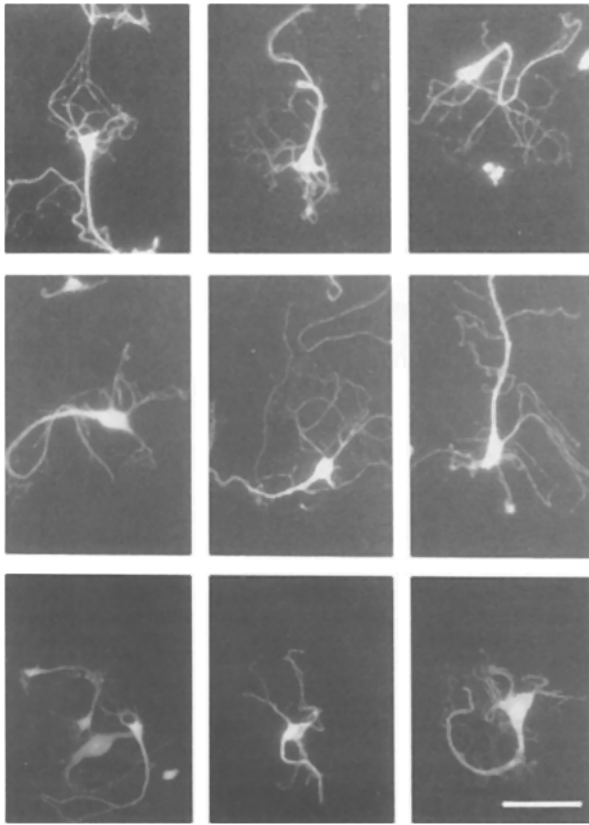


**Figure 2.** Neurons isolated from frozen brain tissue by the technique outlined in Materials and Methods during the early preparative stages before collagenase digestion. Neurons in the top and bottom panels were stained with carbocyanine D272, and those in the middle panels with the carbocyanine D378. These cationic lipophilic probes have a high quantum yield and a high affinity for membranes that produces remarkable detail of the cell membrane and underlying organelles. In addition, the very fine resolution of these fluorochromes also permits the identification and visualization of the detailed morphology of neurites, including varicosities and appendages. Bar, 60  $\mu\text{m}$ .

respective cells during the digestion. Additionally, a small proportion of cells was also destroyed. Release of DNA caused some clumping, a phenomenon avoided by the use of DNase I. At all experimental steps in this study we estimated the quality and composition of our preparations by carbocyanine staining. This technique, outlined in Materials and Methods, permits a very rapid and refined assessment of the cellular structures, as shown in Fig. 2. No major staining differences were found between the two carbocyanines used in this study.

Complete disintegration and solubilization of cellular structures was achieved by the use of SDS. After washing away the soluble fraction, the only remaining insoluble materials were PHF cytoskeletons, lipofuscin granules, and a small amount of insoluble cell debris. Mixed with these insoluble structures were the APCP. Because of their insolubility, size, and density, these proteins copurified with the neuronal population during the course of their isolation. A final purification step using sucrose density gradient centrifugation yielded a series of discrete bands of highly enriched PHF cytoskeletons and amyloid cores, whose composition

was described in Materials and Methods. As can be seen in Figs. 3–5, most of the PHF cytoskeletons still retained their cellular shape and, in some cases, surrounded a central “cavity,” which was previously occupied by the nerve cell nucleus. The only contaminant in our best preparations consisted of a small amount of lipofuscin granules entrapped within the PHF cytoskeletal network (Fig. 4). Those interfaces rich in amyloid cores were very homogenous also, as illustrated in Fig. 6.

Immunofluorescence studies using antiubiquitin, antitau, and antineurofilament antibodies revealed that each of these antigenic epitopes was present on the purified PHF cytoskeletons, as shown in Fig. 7. Moreover, we questioned whether these antigens, specifically tau and neurofilament, were carried by all PHFs simultaneously. Dual labeling immunofluorescence studies using FITC- and TRITC-coupled second antibody indicated that there were heterogeneous populations of PHF in terms of the presence of tau and neurofilament proteins. Although a majority of PHFs demonstrated dual fluorescence, clearly many PHFs were only weakly positive or entirely negative for one or both antigens. Similar observations have been reported by other investigators in other PHF preparations (17, 56).

The total amino acid composition of our best PHF preparations, which we conservatively estimated to be 95% pure, is given in Table II. The composition differed substantially ( $P = 0.002$ ) from those published for the APCP, both by ourselves (51) and by others (36, 54). Glycine, glutamic acid, and lysine appeared to be the three most abundant amino acids.

The highly enriched PHF cytoskeletal and APCP fractions were purified further by solubilization in concentrated formic acid, followed by dialysis against 6 M  $\text{GHCl}$ . We found that, even in the presence of the latter denaturing agent, the APCP components repolymerized into variable length filamentous structures measuring 10 nm in diameter which formed aggregates very similar to those observed before depolymerization (Fig. 8). In addition, the repolymerized APCP was negative for ubiquitin, tau, and neurofilament antigens, as they also were in situ and before depolymerization. Furthermore, the amino acid composition of this fraction (Table II) highly resembled that previously obtained in our laboratory for the APCP, when these structures were purified by fluorescence-activated cell sorting (51).

In contrast, the components of the PHF cytoskeletons remained soluble during the transition from formic acid to 6 M  $\text{GHCl}$ . An aliquot of this material was directly tested for the presence of ubiquitin, tau, and neurofilament epitopes. All three antigens were present in this fraction by dot blot assay. Attempts to repolymerize the PHF by removing the  $\text{GHCl}$  by dialysis against either 0.5% ammonium bicarbonate or 1.5% formic acid failed to recreate the native characteristics of the bi-filar, intertwined (helical) structure of the PHFs. Instead, we observed aggregates of protein which showed, at their periphery, both short, reticularlike structures and a more condensed heterogeneous filamentous component.

Size exclusion chromatography of the formic acid/6 M  $\text{GHCl}$ -solubilized PHF peptides yielded five discrete peaks (Fig. 9 A). The  $M_r$  of fractions 1–3 were 200,000, 9,000, and 4,500, respectively. Fractions 4 and 5 had a longer retention time than the neurotensin marker ( $M_r$ , 1,700) and therefore their  $M_r$  could not be assigned. The amino acid composi-

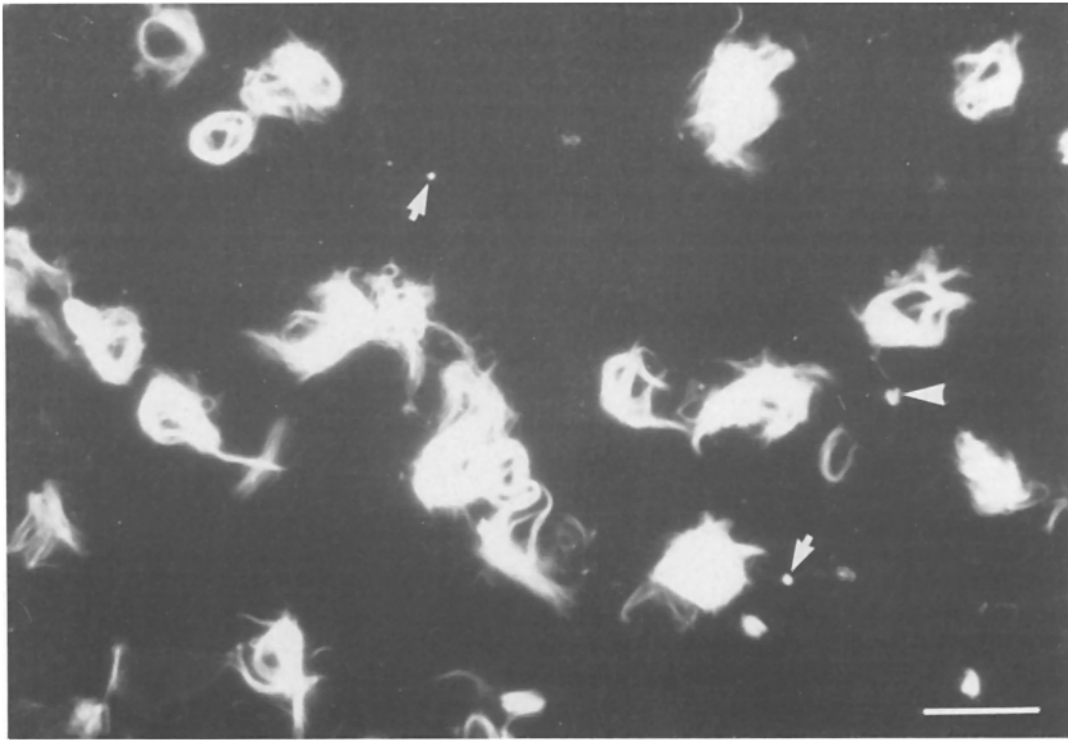


**Figure 3.** Thioflavine T-stained PHF cytoskeletons obtained from 2.1/2.0-M sucrose interface shown in Fig. 3. This layer contained more than 90% PHF cytoskeleton (assessed by fluorescence and electron microscopy). A small amount of lipofuscin granules (*arrows*) and some small specks of APCP (*arrowhead*) still contaminated the specimen. Acid thioflavine T staining was chosen (over thioflavine S or Congo red) because when the specimens were excited at 370 nm, the APCP fluoresced in blue (emission, 420 nm), and the PHF cytoskeletons in green-yellow (emission, 520 nm). The autofluorescence of lipofuscin was also differentiated (emission, 450 nm). Hence, besides their morphology, all those structures were clearly distinguished by fluorescence microscopy. Bar, 20  $\mu$ m.

tions of these polypeptides are given in Table III. Fractions 2 and 3 appear to be highly related in composition and  $M_r$ , suggesting that fraction 2 may be a dimer of fraction 3. These molecules are rich in Gly, Glu, Ser, and Asp. Although fractions 1 and 4 also resemble one another, having Gly, Gly, Asp, and Ser as their more abundant amino acids, nevertheless, important differences must exist between these two proteins. Fraction 1 is the only one in the entire set which proved positive for ubiquitin, tau, and neurofilament by immunodot blot technique. Amino acid analysis also permitted the direct calculation of the molar ratio among the five components. Fraction 4 appears to contain most of the protein (64%) followed by fraction 1 (18%).

Size exclusion chromatography of formic acid/6 M  $\text{GHCl}$ /formic acid-solubilized APCP peptides also rendered five major fractions (Fig. 9 B) with an apparent  $M_r$  of 200,000, 33,000, 10,000, 5,000, and an undetermined  $M_r$  for peak 5. The amino acid compositions of fractions 3 and 4 revealed a close relationship, which suggested fraction 3 was a dimer of fraction 4 (Table IV). Furthermore, it is fraction 4 (representing 57% of the total APCP) that appears to correspond to the sequenced 42-amino acid peptide of the  $\beta$ -amyloid (13, 36, 37). By contrast, fractions 1 and 2 (representing 15 and 4%, respectively) resembled one another more closely than they did either fraction 3 or 4. Among others, the most striking differences are in the values of Thr, Pro, Val, and Arg. In addition, the peptides obtained from the APCP size exclusion chromatography were negative when stained with

antibodies to ubiquitin, tau, and neurofilament by immunodot blot.

### Discussion

In a recent review entitled "Alzheimer's Disease: Its Proteins and Genes," Glenner (12) stressed that in spite of the fact that the PHFs of this degenerative disease have been the subject of intense investigation for over 15 years, their chemical nature still "remains ill defined." Until now, two principle reasons have precluded a more definitive advance in this area: (a) the inability to obtain appropriately pure specimens of PHF in quantities adequate to allow further biochemical characterization, and (b) the problem of PHF insolubility. In this paper we have presented a protocol which described the isolation of neuronal PHF of very high purity and in sufficient quantity to permit further biochemical characterization. Such studies will help to determine the intrinsic composition of these structures.

With the exception of Iqbal et al. (25) who, in 1974, attempted to purify PHF from isolated neurons, previous methodologies (26, 27, 36, 37, 53, 54) aimed at obtaining purified PHF fractions used, among others, early homogenization of the brain by detergents in the presence of reducing agents and, in some cases, the use of proteolytic enzymes or even high temperature treatment. We devised a technique that avoided these potentially detrimental procedures (6, 23, 45). The preservation of intact neurons up to the final Percoll



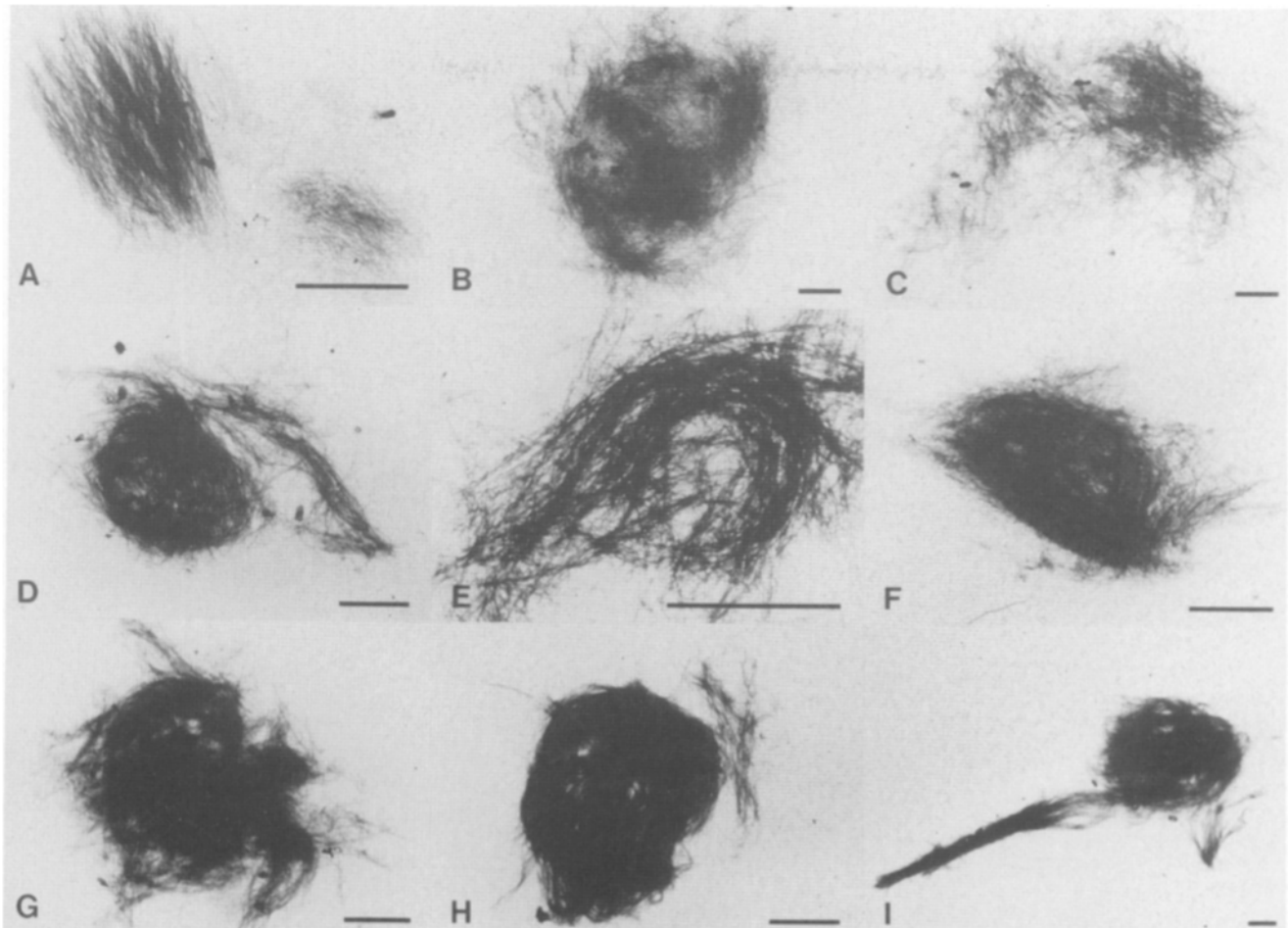


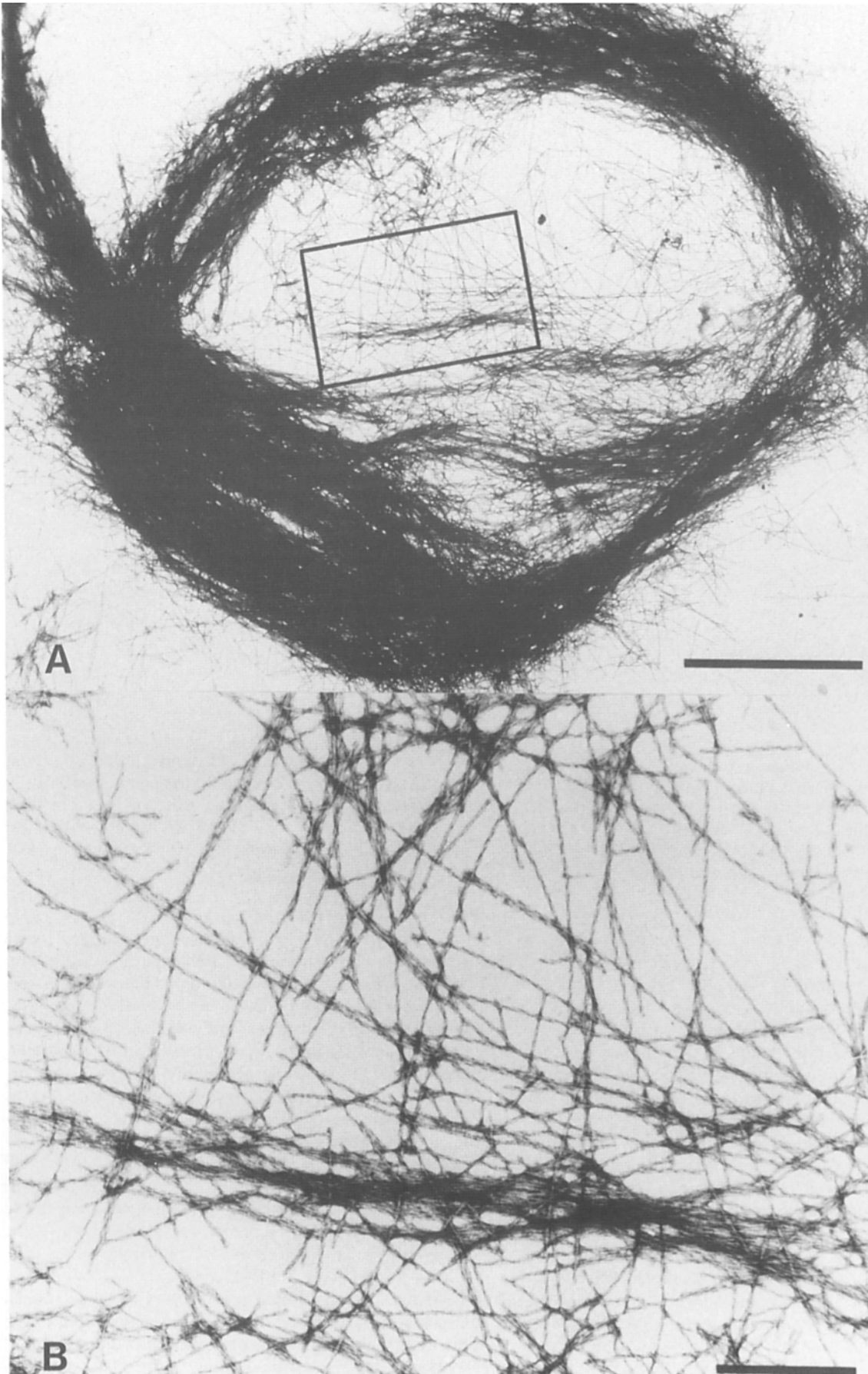
**Figure 4.** Electron micrographs showing a series of PHF cytoskeletons. (A–F) PHF cytoskeletons obtained from the 2.0/1.7-M sucrose interface, which were further purified by low speed centrifugation in 1 M sucrose, as described in the text. (G–I) PHF cytoskeletons from the 2.1/2.0-M sucrose interface. Notice the larger and more compact network of the latter. The cytoskeletons still preserve what appeared to be their previous cellular (body) shape. In some instances a central “cavity” is distinguished (see also Figs. 3 and 5) that was probably occupied by the former nucleus of the intact cell. In some other cases, elongated appendages of PHF depart from a larger globular mass of PHF, suggesting an apical dendrite (I). Some small granules of lipofuscin can be seen entrapped within the PHF network. Bars, 5  $\mu$ m.

fractionation helps to avoid initial contamination of PHF by extracellular ACP and other cellular debris.

In spite of being frozen at  $-70^{\circ}\text{C}$  for five years, cellular integrity was well preserved (Fig. 2). Several factors used in the present protocol may have contributed to their preservation. Among them was the initial slicing and mincing of the brain at low temperature in an isotonic medium containing protease inhibitors, as well as the very gentle sieving of the tissue through decreasing size stainless steel meshes. Although the cells were treated with hypertonic sucrose solutions, they were exposed to these conditions for the minimum time necessary followed by immediate return to isotonic medium. We recognize, however, that mechanical trauma and the necessary chemical steps, as well as the inability of the cells to regenerate, were an important source of neuronal damage during the isolation procedure. Nevertheless, from an initial 2,000 g of cortex, we recovered 50 ml of cells (settled at unit gravity), of which 90% were neurons, from our Percoll interfaces and a final volume of  $\sim 150$   $\mu$ l of purified PHF cytoskeletons.

In a previous series of experiments, we used the fluores-

cence-activated cell sorter (FACS) as the final step in the purification of PHF cytoskeletons. FACS purification, as also experienced by other laboratories (24, 40), was only partially successful. When reacted under acidic conditions, thioflavine T distinctly labeled PHF cytoskeletons and ACP, while the autofluorescent lipofuscin remained unlabeled. Separation of these elements occurred in the FACS when excited at 370 nm. To label these structures, however, it was necessary to remove the detergent (SDS). This caused a significant aggregation of cores and tangles, which was very difficult to dissociate even after the SDS was reincorporated in the buffer. We estimated that the maximum purity of PHF cytoskeletons attainable through FACS amounted to no more than 70%. By using the technique presented in this paper, the degree of purity in our best PHF preparations was 95% or more. At EM level, the 5% contamination consisted of some granules of lipofuscin entrapped within the isolated PHF cytoskeleton network, and a negligible amount of ACP in the form of small but very prominent protein aggregates. Moreover, electron microscopy of the isolated PHF cytoskeletons showed them to be homogeneously composed of PHF,





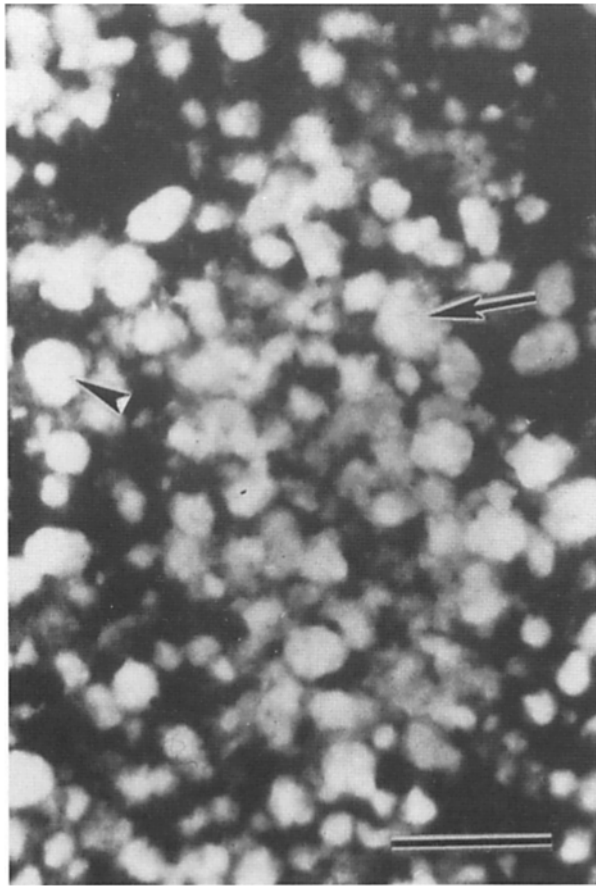


**Figure 6.** Amyloid plaque protein cores stained with thioflavine T. These cores were obtained from the 1.7/1.4-M sucrose density gradient interface. Thioflavine T staining, when excited at 370 nm, distinguishes two discrete types of amyloid cores: intensely glowing silver blue (*arrowhead*) and deep dark blue (*arrow*). We suggest that these differences in staining characteristics may be due to small chemical inequality either in protein composition or posttranslational modification (such as glycosylation and phosphorylation). A second possibility is that they simply represent differences in filament concentration. However, in a random sample of cores, like the one shown in this figure, a continuous distribution of fluorescent tones is rarely seen. Bar, 10  $\mu\text{m}$ .

as established by filament measurements of 20–24-nm diameter and 70-nm axial periodicity.

As the data presented in Table II clearly show, the amino acid composition of PHF substantially differed from APCP and lipofuscin molecules. The relative amounts of eight amino acids (Pro, Thr, Met, Arg, Lys, Phe, Ser, and Ala) differed by more than 40%, when the values of PHF and APCP were compared. The most represented amino acids in the PHF were Gly, Glu, Lys, and Asp, while in the APCP they were Gly, Val, Glu, and Ala. These results strongly suggest a

different protein composition and quite possibly a different pathogenesis as well. When compared to the PHF amino acid compositions published by others (36, 54), important deviations, which could have resulted from different degrees of contamination, were apparent. The issue of whether or not identity exists between the polypeptide composition of the intraneuronal PHFs and the extracellular APCP has not been settled. On the one hand, Masters et al. (36) and Guirouy et al. (19) support the concept of identity based on amino acid sequence data between AD-PHF and AD-APCP and between the AD-PHF and PHF obtained from patients who died of Parkinson dementia complex of Guam. This latter degenerative disease is purportedly free of neuritic plaques and, therefore, should not contribute a potential APCP contamination during the isolation procedures. On the other hand, highly purified or enriched PHFs seem to carry an assortment of antigenic epitopes that were encountered in other proteins like ubiquitin (43, 48, 56), tau (18, 35, 44, 56, 72), neurofilaments (2, 10, 39, 41, 47) and other microtubule-associated proteins (34, 47). The purification scheme described here permitted the conservation of some of these epitopes, which suggests they may be “intrinsic” components of AD-PHF. Moreover, to the best of our knowledge, antibodies raised against either PHF or APCP do not show cross-reactivity (54). This also suggests nonidentity between the two types of filaments.

The results of the chemical depolymerization studies showed that lipofuscin granules seem to be chemically stable on brief exposure to concentrated formic acid and, therefore, can be eliminated by centrifugation. By contrast, PHF and APCP are apparently depolymerized by formic acid and are probably disrupted to random coils. Upon removal of formic acid by dialysis against 6 M  $\text{GHCl}$ , PHF polypeptides remained in solution whereas APCP repolymerized. It could be argued that the very hydrophobic nature of the APCP induces the regeneration of its supramolecular structure, even in the presence of a hydrophilic strong electrolyte. This important thermodynamic behavior suggests major physicochemical differences between the structures of APCP and PHF.

Similarly, the amino acid composition of the APCP and PHF proteins obtained after fractionation by size exclusion chromatography demonstrate significant differences. In support of these compositional deviations, which have been highlighted in Results, are the stoichiometric differences within and between the fractions separated by the two chromatographic steps. The most representative APCP fraction is fraction 4, accounting for 57% of the entire sample, with an apparent  $M_r$  of  $\sim 5,000$ . With some minor deviations, this peak closely corresponds to the  $\beta$ -amyloid protein. On the other hand, the most representative fraction in the PHF preparation, with an estimated 64% of the total sample, appears after the 1,700- $M_r$  marker. Either this peptide has an anomalous retention time in the TSK 3000 SW column (Beckman Instruments, Inc., Altex Division) or this fraction is

**Figure 5.** Higher magnification electron micrograph of a PHF cytoskeleton showing a homogeneous composition. The outlined area (A) has been enlarged in the bottom panel (B). PHF appear in a random array as unbranched filaments with well-defined profiles and with no other discernable structures in the background. Their apparent straight rigidity may be the result of their helical configuration in contrast to the very flexible “monofilamentous” structures of APCP. On methodical and careful screening of PHF cytoskeletons at high magnification, no filaments other than PHF were observed. Bars: (A) 3  $\mu\text{m}$ ; (B) 0.5  $\mu\text{m}$ .

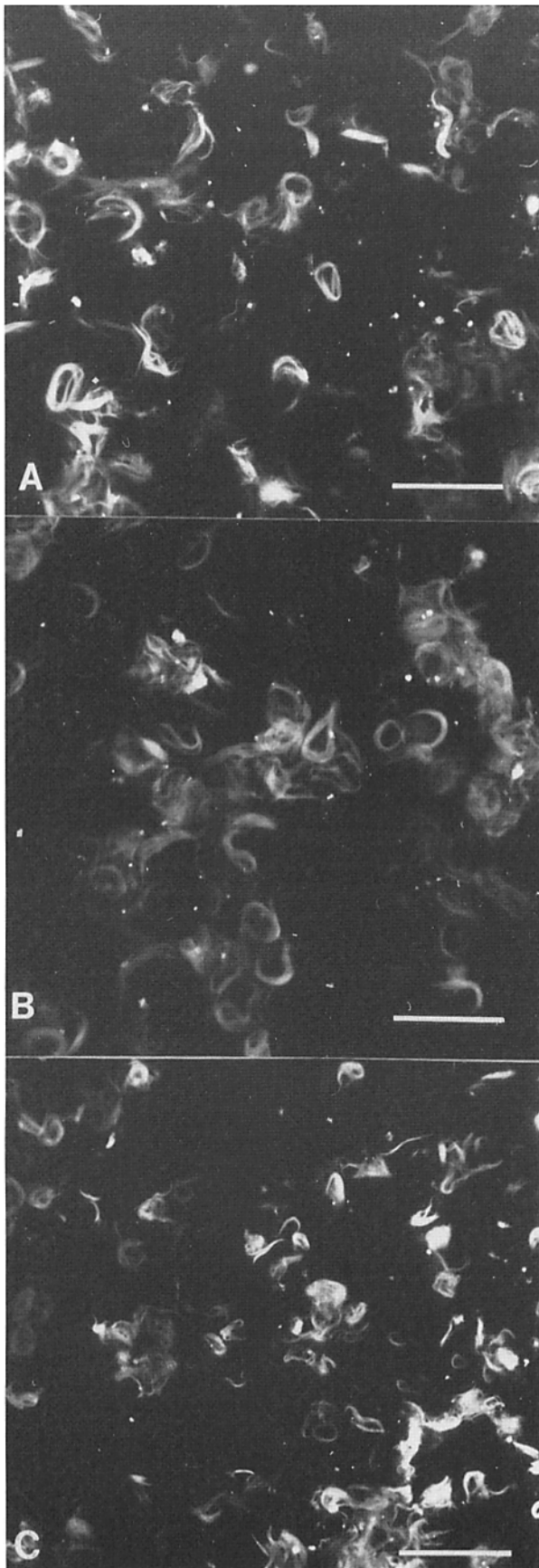


Table II. Amino Acid Compositions of PHF Cytoskeletons, APCP, and Lipofuscin\*

Amino acid	PHFs‡ (mol/100 residues)	APCP‡ (mol/100 residues)	Lipofuscin (mol/100 residues)
Cys	ND	0.8§	16.3§
Asp	9.0	8.1§	8.2§
Met	1.1	2.7	1.5
Thr	5.0	1.4	4.1
Ser	8.8	4.8	6.4
Glu	10.7	9.6	7.8
Pro	4.0	1.1	2.7
Gly	12.7	15.5	12.5
Ala	5.1	8.8	6.3
Val¶	8.8	14.3	8.1
Ile¶	5.2	6.5	4.3
Leu	6.6	6.1	7.7
Tyr	2.6	1.7	2.3
Phe	3.3	6.3	5.1
His	3.5	5.0	0.9
Lys	9.3	5.2	3.3
Arg	4.3	2.1	2.5
Trp	ND	ND	ND

\* Average values from determinations at 24, 48, and 72 h of hydrolysis, except as noted.

‡ Highly significant differences between PHF and APCP; Chi-square = 33.780,  $P = 0.002$ .

§ Quantitated as cystic acid and methionine sulfone after performic acid oxidation.

|| Extrapolated to 0 h hydrolysis value.

¶ 72 h hydrolysis value.

composed of 2–3 peptides of similar size. If the former alternative applies, one could assume a peptide with a minimum length of 31–33 amino acid residues, as calculated from the peak's amino acid analysis molar ratios. Next in representation is the PHF fraction 1 (18%). This peak, which elutes with an  $M_r$  of  $\sim 200,000$ , resembles fraction 4 in amino acid composition. Therefore, the possibility of this being an aggregated form of the major fraction 4 exists. However, fraction 1 is the only one in the entire set of TSK 3000 SW-separated peptides that is immunochemically positive for ubiquitin, tau, and neurofilament epitopes. Last is the high degree of similarity that exists among PHF fractions 2, 3, and 5, with peak 5, again, possibly representing an anomalously retained peptide.

Of particular interest was the proteolytic signal protein ubiquitin (76 amino acids long), which appeared to be intimately associated and perhaps covalently linked to the PHF polypeptides, since it continued to be present even after the repolymerization procedure. Mori et al. (43) have isolated from PHF preparations peptides that correspond to two internal sequences of ubiquitin.

The primary goal in devising a technique that would permit large-scale purification of brain cells from suitable AD postmortem material was that, in the absence of an animal

Figure 7. Immunofluorescence reactivity of PHF cytoskeletons derived from the 2.0/1.7-M sucrose interface, stained by indirect immunofluorescence with FITC-conjugated second antibody. (A) Anti-ubiquitin; (B) antitau; (C) antineurofilament (8D8 antibody). Bars, 30  $\mu$ m.

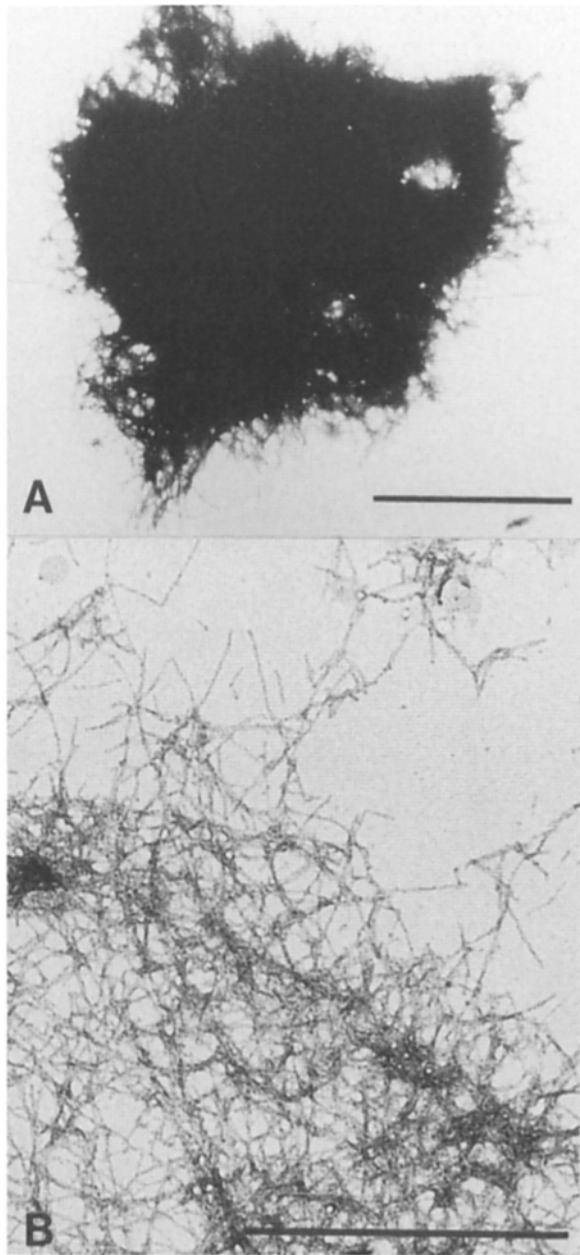


**Figure 8.** Electron micrographs of stained APCP. APCPs are formed by the compact aggregation of filaments, measuring 10 nm in diameter, which appear flexible. (A) A dense amyloid core purified by the present protocol. (B) After treatment with concentrated formic acid for 2 h at room temperature, the specimen was diluted with 50 vol of water and lyophilized. APCPs were resuspended in 50 mM Tris-HCl, pH 7.5, 0.2% SDS. An aliquot of this specimen was sonicated and a drop was deposited onto a Formvar-coated copper grid. After 3 min, excess buffer was drained away by filter paper. The grid was washed three times with water and stained with 1% aqueous uranyl acetate for 4 min. The repolymerized APCP appeared as a network of 10-nm filaments morphologically indistinguishable from those shown at the periphery in A. Bars, 1.0  $\mu$ m.

model, access to pathological neurons would allow for a more selective investigation of the cellular pathophysiology of AD at different stages of its evolution. Of immediate particular interest was the suggestion of a reciprocal relationship

**Table III. Amino Acid Composition of Alzheimer's Disease Paired Helical Filament Proteins**

	Size exclusion HPLC on a TSK 3000 SW column				
	Peak 1	Peak 2	Peak 3	Peak 4	Peak 5
	$M_r$ 200,000	$M_r$ 9000	$M_r$ 4500	$M_r$ --	$M_r$ --
	<i>mol %</i>	<i>mol %</i>	<i>mol %</i>	<i>mol %</i>	<i>mol %</i>
Cys	ND	ND	ND	ND	ND
Asp	11.3	8.7	8.4	10.5	8.3
Thr	4.2	3.1	3.6	3.1	3.7
Ser	10.5	13.3	13.9	10.6	12.9
Glu	21.0	17.2	17.6	24.3	17.2
Pro	4.0	3.1	3.4	3.3	3.8
Gly	15.5	22.0	21.6	16.1	20.4
Ala	7.2	7.9	7.6	6.5	8.2
Val	5.7	6.0	5.0	5.9	4.9
Met	0.6	—	—	—	—
Ile	2.7	2.9	2.9	3.1	3.2
Leu	5.0	4.4	5.2	5.8	6.3
Tyr	1.3	0.9	1.0	1.0	0.6
Phe	1.9	2.7	2.7	2.6	2.3
His	1.6	2.0	1.2	1.6	1.6
Lys	4.7	3.0	3.1	3.1	3.5
Arg	2.8	2.8	2.8	2.5	3.1
Trp	ND	ND	ND	ND	ND

between the disappearance of microtubules and neurofilaments and the appearance of PHF cytoskeletons, which appear to carry epitopes of the former structures. We believe that these two phenomena are related (16). Great emphasis has been put upon the characterization of PHF, partly because, with the exception of those seen in aging, they are alien to the normal neuron and because they appear in such profusion. However, of equal importance is the question of

**Table IV. Amino Acid Composition of Alzheimer's Disease Amyloid Plaque Core Proteins**

	Size exclusion HPLC on a Superose 12 column				
	Peak 1	Peak 2	Peak 3	Peak 4	Peak 5
	$M_r$ 200,000	$M_r$ 33,000	$M_r$ 10,000	$M_r$ 5,000	$M_r$ --
	<i>mol %</i>	<i>mol %</i>	<i>mol %</i>	<i>mol %</i>	<i>mol %</i>
Cys	ND	ND	ND	ND	ND
Asp	8.7	9.6	8.2	8.1	8.0
Thr	4.7	4.4	0.8	0.3	2.6
Ser	8.1	6.8	5.2	4.8	6.7
Glu	10.8	12.9	10.8	9.9	9.8
Pro	4.6	3.9	0.7	0.2	4.5
Gly	12.3	11.6	16.5	16.1	21.6
Ala	7.9	9.4	9.3	9.1	9.5
Val	7.5	7.5	14.2	14.5	7.6
Met	2.3	2.0	2.1	2.7	1.8
Ile	4.4	4.2	6.0	6.0	4.3
Leu	8.0	8.7	5.8	5.7	5.3
Tyr	3.2	2.9	2.7	2.6	4.1
Phe	3.7	3.8	5.9	6.8	3.5
His	3.0	2.7	5.9	6.8	3.6
Lys	4.4	4.1	3.7	4.5	2.5
Arg	6.4	5.5	2.2	1.9	4.6
Trp	ND	ND	ND	ND	ND

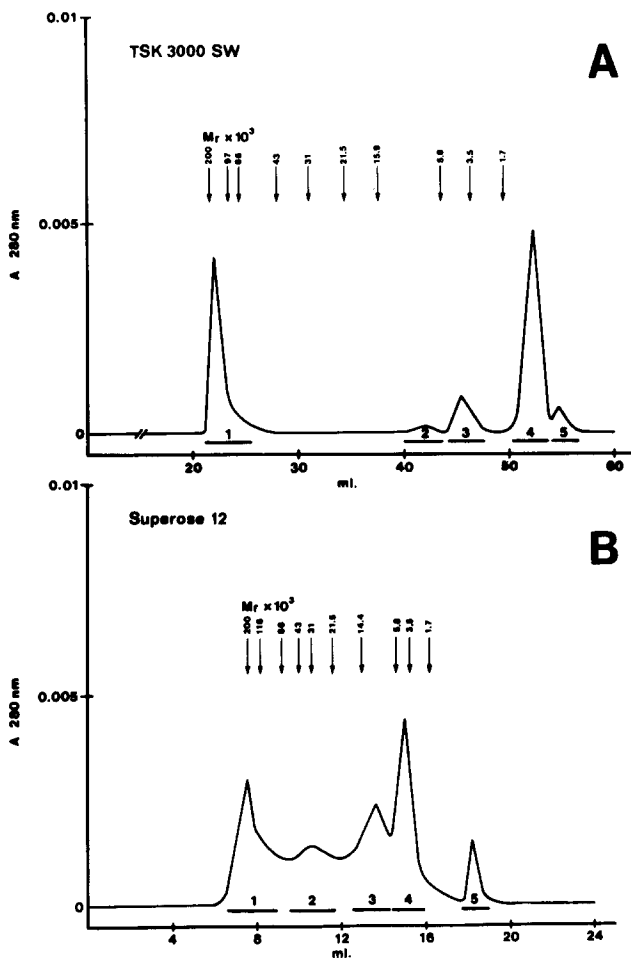


**Figure 9.** Chromatographic profiles of PHF and ACP peptides. (A) Size exclusion chromatography of PHF on a TSK 3000 SW column (7.5 × 600 mm; Beckman Instruments, Altex Division) equipped with a guard column (75 × 7.5 mm; Altex Scientific Inc.) containing the same bed material, equilibrated with 6 M GHCl containing 5% formic acid. The chromatography was developed at a flow rate of 0.5 ml/min and monitored at 280 nm. The column was calibrated, using the same denaturing solvents as described above, with 10 different proteins and peptides of known  $M_r$ : myosin, phosphorylase B, BSA, ovalbumin, carbonic anhydrase, soybean trypsin inhibitor, hemoglobin  $\beta$ -chain, insulin, glucagon, and neurotensin. 300- $\mu$ l aliquots of solubilized PHFs were centrifuged at 250,000  $g$  for 20 min before loading onto the column. PHFs resolved into five different peaks with  $M_r$ s of  $\sim$ 200,000 (peak 1), 9,000 (peak 2), 4,500 (peak 3); peaks 4 and 5 eluted after the 1,700 marker. The amino acid compositions of these fractions is shown in Table III. The yield in nmol for each of the fractions permitted the calculation of their relative fractional representation as 18, 4, 6, 64, and 8%, respectively. Immunodot blot analyses indicated that only the protein eluted in peak 1 contained ubiquitin, tau, and neurofilament epitopes. (B) Size exclusion chromatography of ACP on a Superose 12 column (10 × 300 mm; Pharmacia Fine Chemicals, Piscataway, NJ) equilibrated with 70% formic acid. The column was calibrated with known standards in 70% formic acid, as described above, with the exception that the hemoglobin  $\beta$ -chain was replaced by lysozyme. Before loading, the ACPs were dialyzed again: 70% formic acid, followed by centrifugation at 250,000  $g$  for 2 min. Aliquots of 300  $\mu$ l were loaded and the chromatography developed at a flow rate of 0.2 ml/min. Each of the five fractions was represented as follows: peak 1 =  $M_r$  200,000 (15%); peak 2 =  $M_r$  33,000 (4%); peak 3 =  $M_r$  10,000 (22%); and peak 4 =  $M_r$  5,000 (57%). Peak 5, with an undetermined  $M_r$ , represented only 2%

why some of the normal cytoskeletal components disappear. This severely compromises vital neuritic transport which, in the ultimate instance, terminates the propagation of action potentials.

It is noteworthy that the  $\beta$ -amyloid protein obtained from the neuritic plaques of AD appear to be more insoluble than the  $\beta$ -protein deposited around blood vessels in the amyloid angiopathy of AD. This latter protein can be isolated under milder conditions (13), readily penetrates acrylamide gels, and is accessible to routine reverse-phase chromatography (46). If both  $\beta$ -proteins have the same amino acid sequence, then posttranslational changes, such as the large amounts of racemized amino acids found in the ACP (55), may confer on this amyloid different conformational characteristics rendering it more insoluble and prone to aggregation.

A plausible interpretation of the accumulation of PHFs may have to do with their insolubility. x-ray diffraction analysis of PHF supports this issue since their predominant molecular structure is that of an antiparallel  $\beta$ -pleated sheet conformation (32). The most favored composition of residues between  $\beta$ -sheet interfaces makes the contact surfaces very stable and hydrophobic, bringing their interactions close to the minimum free energy conformation (8). In addition, the in vitro resistance that PHF show to a wide variety of proteolytic enzymes supports this line of reasoning (51, 53). Partial enzymic hydrolysis seems to take place only after PHFs were subjected to the powerful denaturing action of concentrated formic acid (43). At this point, the suggestion could be made that PHF accumulation represents a failure in the ubiquitin-mediated proteolysis. This failure could occur as the result of steric hindrance. Alternatively, some hydrolysis could occur but PHF degradation and dissociation might be inhibited because its tertiary and quaternary structures are thermodynamically very stable.

The techniques and information advanced in this paper should directly provide a better understanding of this filamentous pathology and may ultimately furnish a view into the etiopathogenesis of the dementing process in Alzheimer's disease.

We are grateful to the Dementia Study Group of the University of Western Ontario and to Drs. C. Gibson and D. Perl for their encouragement and generous support. We also extend our gratitude to Drs. S. Ghandour and J. Benjamins for the gift of antibodies against glial cells. Drs. C. Anderson, G. Perkins, J. V. Frei, M. D. Silver, and A. C. Wallace kindly provided access to pathological tissues. We are in debt to L. Bale, J. Burton, J. MacGregor, S. Griffin-Brooks, E. Ojalvo-Rose, and J. Little for their excellent technical assistance and to M. Kukuruga for skillful assistance in the use of the fluorescence activated cell sorter.

This work was supported in part by National Institutes of Health grants HL32870 (K. C. Palmer), AG03047 (M. J. Ball), and AG07470 and GM-35803 (V. Chau), and by the Atkinson Charitable Foundation of Toronto (M. J. Ball).

Received for publication 15 July 1988 and in revised form 13 September 1988.

#### References

1. Anderton, B., and C. Miller. 1986. Proteins in a twist: are neurofibrillary tangles and amyloid in Alzheimer's disease composed of the same pro-

The amino acid compositions of these fractions is given in Table IV. Immunodot blot indicated all five peaks positive for the anti- $\beta$ -amyloid protein (kindly provided by Dr. D. Selkoe).

- tein? *Trends Neurosci.* 9:337-338.
2. Anderton, B. H., D. Breinburg, M. J. Downes, P. J. Green, B. E. Tomlinson, J. Ulrich, J. N. Wood, and J. Kahn. 1982. Monoclonal antibodies show that neurofibrillary tangles and neurofilaments share antigenic determinants. *Nature (Lond.)*. 289:84-86.
  3. Bahmanyar, S., G. A. Higgins, D. Goldgaber, D. A. Lewis, J. H. Morrison, M. G. Wilson, S. K. Shankar, and D. C. Gajdusek. 1987. Localization of amyloid  $\beta$  protein messenger RNA in brains from patients with Alzheimer's disease. *Science (Wash. DC)*. 237:77-80.
  4. Ball, M. J., V. Hachinski, A. Fox, A. J. Kershen, M. Fisman, W. Blume, V. A. Kral, H. Fox, and H. Merskey. 1985. A new definition of Alzheimer's disease: a hippocampal dementia. *Lancet*. 1:14-16.
  5. Ball, M. J., S. Griffin-Brooks, J. MacGregor, B. Nagy, E. Ojalvo-Rose, and P. H. Fewster. 1988. Neuropathological definition of Alzheimer disease: multivariate analyses in the morphometric distinction between Alzheimer dementia and normal aging. *Alzheimer Disease and Associated Disorders*. 2:29-37.
  6. Bjarnason, J., and K. J. Carpenter. 1970. Mechanisms of heat damage in proteins. 2. Chemical changes in pure proteins. *Br. J. Nutr.* 24:313-329.
  7. Blake, M. S., K. H. Johnston, G. J. Russell-Jones, and E. C. Gotschlich. 1984. A rapid, sensitive method for detection of alkaline phosphatase-conjugated anti-antibody on Western blots. *Anal. Biochem.* 136:175-179.
  8. Chothia, C. 1984. Principles that determine the structure of proteins. *Annu. Rev. Biochem.* 53:537-572.
  9. Cohen, M. L., T. E. Golde, M. F. Usiak, L. H. Younkin, and S. G. Younkin. 1988. In situ hybridization of nucleus basalis neurons shows increased  $\beta$ -amyloid mRNA in Alzheimer disease. *Proc. Natl. Acad. Sci. USA*. 85:1227-1231.
  10. Cork, L. C., N. H. Sternberger, L. A. Sternberger, M. F. Casanova, R. G. Struble, and D. L. Price. 1986. Phosphorylated neurofilament antigens in neurofibrillary tangles in Alzheimer's disease. *J. Neuropathol. & Exp. Neurol.* 45:56-64.
  11. Corsellis, J. A. N., C. J. Bruton, and D. Freeman-Browne. 1973. The aftermath of boxing. *Psychol. Med.* 3:270-303.
  12. Glenner, G. G. 1988. Alzheimer's disease: its proteins and genes. *Cell*. 52:307-308.
  13. Glenner, G. G., and C. W. Wong. 1984. Alzheimer's disease: initial report of the purification and characterization of a novel cerebrovascular amyloid protein. *Biochem. Biophys. Res. Commun.* 120:885-890.
  14. Goedert, M. 1987. Neuronal localization of amyloid beta protein precursor mRNA in normal human brain and in Alzheimer's disease. *EMBO (Eur. Mol. Biol. Organ.) J.* 6:3627-3632.
  15. Goldgaber, D., M. T. Lerman, O. W. McBride, U. Safiotti, and D. C. Gajdusek. 1987. Characterization and chromosomal localization of a DNA encoding brain amyloid of Alzheimer's disease. *Science (Wash. DC)*. 235:877-880.
  16. Gray, E. G., M. Paula-Barbosa, and A. Roher. 1987. Alzheimer's disease: paired helical filaments and cytomembranes. *Neuropathol. Appl. Neurobiol.* 13:91-110.
  17. Grundke-Iqbal, I., K. Iqbal, Y. C. Tung, G. P. Wang, and H. M. Wisniewski. 1985. Alzheimer paired helical filaments: cross-reacting polypeptide is normally present in brain. *Acta Neuropathol.* 66:52-61.
  18. Grundke-Iqbal, I., K. Iqbal, M. Qianlan, Y. C. Tung, M. S. Zaidi, and H. M. Wisniewski. 1986. Microtubule-associated protein tau: a component of Alzheimer paired helical filaments. *J. Biol. Chem.* 261:6084-6089.
  19. Guirouy, D. C., M. Miyazaki, G. Multhaup, P. Fischer, R. M. Garruto, K. Beyreuther, C. L. Masters, G. Simms, C. J. Gibbs, and D. C. Gajdusek. 1987. Amyloid of neurofibrillary tangles of Guamanian Parkinsonism-dementia and Alzheimer disease share identical amino acid sequence. *Proc. Natl. Acad. Sci. USA*. 84:2073-2077.
  20. Haas, A. L., and P. M. Bright. 1985. The immunochemical detection and quantitation of intracellular ubiquitin-protein conjugates. *J. Biol. Chem.* 260:12464-12473.
  21. Higgins, G. A., D. A. Lewis, S. Bahmanyar, D. Goldgaber, D. C. Gajdusek, W. G. Young, J. H. Morrison, and M. C. Wilson. 1988. Differential regulation of amyloid- $\beta$ -protein mRNA expression within hippocampal neuronal subpopulations in Alzheimer disease. *Proc. Natl. Acad. Sci. USA*. 85:1297-1301.
  22. Hirano, A. 1970. Neurofibrillary changes in conditions related to Alzheimer's disease. *Ciba Symp.* 185-201.
  23. Hurrell, R. F., and K. J. Carpenter. 1977. Nutritional significance of cross-link formation during food processing. In *Protein cross-linking*. M. Friedman, editor. Plenum Publishing Corp., NY. 225-238.
  24. Hussey, S., C. M. Yates, and G. Fink. 1986. Fluorescence activated cell sorting (FACS) as a separation method for neurofibrillary tangles in Alzheimer's disease. *J. Neurosci. Methods*. 16:1-8.
  25. Iqbal, K., H. M. Wisniewski, M. L. Shelansky, S. Brostoff, B. H. Liwnics, and R. Terry. 1974. Protein changes in senile dementia. *Brain Res.* 77:337-343.
  26. Iqbal, K., T. Zaidi, C. H. Thompson, P. A. Merz, and H. M. Wisniewski. 1984. Alzheimer paired helical filaments: bulk isolation, solubility, and protein composition. *Acta Neuropathol. (Berl.)*. 62:167-177.
  27. Iqbal, K., I. Grundke-Iqbal, T. Zaidi, N. Ali, and H. M. Wisniewski. 1986. Are Alzheimer neurofibrillary tangles insoluble polymers? *Life Sci.* 38:1695-1700.
  28. Kang, J., H. G. Lemaire, A. Unterbeck, J. M. Salbaum, C. L. Masters, K. H. Grzeschik, G. Multhaup, K. Beyreuther, and B. Muller-Hill. 1987. The precursor of Alzheimer's disease amyloid A4 protein resembles a cell surface receptor. *Nature (Lond.)*. 325:733-736.
  29. Khachaturian, Z. S. 1985. Diagnosis of Alzheimer's disease. *Arch. Neurol.* 42:1097-1105.
  30. Kidd, M. 1963. Paired helical filaments in electron microscopy of Alzheimer's disease. *Nature (Lond.)*. 197:192-193.
  31. Kidd, M. 1964. Alzheimer's disease: an electron microscope study. *Brain*. 87:307-320.
  32. Kirschner, D. A., C. Abraham, and D. J. Selkoe. 1986. X-ray diffraction from intraneuronal paired helical filaments and extraneuronal amyloid fibers in Alzheimer disease indicates cross- $\beta$  conformation. *Proc. Natl. Acad. Sci. USA*. 83:503-507.
  33. Kitaguchi, N., Y. Takahashi, Y. Tokushima, S. Shiojiri, and H. Ito. 1988. Novel precursor of Alzheimer's disease amyloid protein shows protease inhibitory activity. *Nature (Lond.)*. 331:530-532.
  34. Kosik, K. S., L. K. Duffy, M. M. Dowling, C. Abraham, A. McCluskey, and D. J. Selkoe. 1984. Microtubule-associated protein 2: monoclonal antibodies demonstrate the selective incorporation of certain epitopes into Alzheimer neurofibrillary tangles. *Proc. Natl. Acad. Sci. USA*. 81:7941-7945.
  35. Kosik, K. S., C. L. Joachim, and D. J. Selkoe. 1986. Microtubule-associated protein tau (T) is a major antigenic component of paired helical filaments in Alzheimer disease. *Proc. Natl. Acad. Sci. USA*. 83:4044-4048.
  36. Masters, C. L., G. Multhaup, G. Simms, J. Pottglessler, R. N. Martins, and K. Beyreuther. 1985. Neuronal origin of a cerebral amyloid: neurofibrillary tangles of Alzheimer's disease contain the same protein as the amyloid of plaque cores and blood vessels. *EMBO (Eur. Mol. Biol. Organ.) J.* 4:2757-2763.
  37. Masters, C. L., G. Simms, N. A. Weinman, G. Multhaup, B. L. McDonald, and K. Beyreuther. 1985. Amyloid plaque core protein in Alzheimer disease and Down syndrome. *Proc. Natl. Acad. Sci. USA*. 82:4245-4249.
  38. Meyer, E. M., C. M. West, and V. Chau. 1986. Antibodies directed against ubiquitin inhibit high affinity [<sup>3</sup>H]choline uptake in rat cerebral cortical synaptosomes. *J. Biol. Chem.* 261:14365-14368.
  39. Miller, C. C. J., J. P. Brion, R. Calvert, T. K. Chin, P. A. M. Eagles, M. J. Downes, J. Flament-Durand, M. Haugh, J. Kahn, A. Probst, J. Ulrich, and B. H. Anderton. 1986. Alzheimer's paired helical filaments share epitopes with neurofilament side arms. *EMBO (Eur. Mol. Biol. Organ.) J.* 5:269-276.
  40. Miller, C. C. J., M. Haugh, B. H. Anderton, L. Hudson, and J. Murphy. 1986. Neurofibrillary tangles from Alzheimer's disease brain purified using a cell sorter. *Neurosci. Lett.* 63:247-252.
  41. Miller, C., M. Haugh, J. Kahn, and B. Anderton. 1986. The cytoskeleton and neurofibrillary tangles in Alzheimer's disease. *Trends Neurosci.* 9:76-81.
  42. Miyakawa, T., A. Shimoji, R. Kuramoto, and Y. Higuchi. 1982. The relationship between senile plaques and cerebral blood vessels in Alzheimer's disease and senile dementia. *Virchows Arch. B Cell Pathol.* 40:121-129.
  43. Mori, H., J. Kondo, and Y. Ihara. 1987. Ubiquitin is a component of paired helical filaments in Alzheimer's disease. *Science (Wash. DC)*. 235:1641-1644.
  44. Nukina, N., and Y. Ihara. 1986. One of the antigenic determinants of paired helical filaments is related to tau protein. *J. Biochem. (Tokyo)*. 99:1541-1544.
  45. Otterburn, M., M. Healy, and W. Sinclair. 1977. The formation, isolation and importance of isopeptides in heated proteins. In *Protein Cross-linking*. M. Friedman, editor. Plenum Publishing Corp., New York. 239-262.
  46. Pardridge, W. M., H. V. Vinters, J. Yang, J. Eisenberg, T. B. Choi, W. W. Tourtellote, V. Heubner, and J. E. Shively. 1987. Amyloid angiopathy of Alzheimer's disease: amino acid composition and partial sequence of a 4,200 Dalton peptide isolated from cortical microvessels. *J. Neurochem.* 49:1394-1401.
  47. Perry, G., N. Rizzoto, L. Autilio-Gambetti, and P. Gambetti. 1985. Paired helical filaments from Alzheimer's disease patients contain cytoskeletal components. *Proc. Natl. Acad. Sci. USA*. 82:3916-3920.
  48. Perry, G., R. Friedman, G. Shaw, and V. Chau. 1987. Ubiquitin is detected in neurofibrillary tangles and senile plaque neurites of Alzheimer's disease brain. *Proc. Natl. Acad. Sci. USA*. 84:3033-3036.
  49. Ponte, P., P. Gonzalez-DeWhitt, J. Schilling, J. Miller, D. Hsu, B. Greenberg, K. Davis, W. Wallace, I. Lieberburg, F. Fuller, and B. Cordell. 1988. A new A4 amyloid mRNA contains a domain homologous to serine proteinase inhibitors. *Nature (Lond.)*. 331:525-527.
  50. Robakis, K. K., H. M. Wisniewski, E. C. Jenkins, E. A. Devine-Gage, G. E. Houck, X. L. Yao, N. Ramakrishna, G. Wolfe, W. P. Silverman, and W. T. Brown. 1987. Chromosome 21q21 sublocalization of gene encoding beta-amyloid peptide in cerebral vessels and neuritic (senile) plaques of people with Alzheimer's disease and Down syndrome. *Lancet*. 1:384-385.
  51. Roher, A., D. Wolfe, M. Palutke, and D. KuKuruga. 1986. Purification, ultrastructure, and chemical analysis of Alzheimer's disease amyloid plaque core protein. *Proc. Natl. Acad. Sci. USA*. 83:2662-2666.

52. Roher, A., E. G. Gray, and M. Paula-Barbosa. 1988. Alzheimer's disease: coated vesicles, coated pits and the amyloid related cell. *Proc. Roy. Soc. Lond. B Biol. Sci.* 232:367-373.
53. Selkoe, D. J., Y. Ihara, and F. J. Salazar. 1982. Alzheimer's disease: insolubility of partially purified paired helical filaments in sodium dodecyl sulfate and urea. *Science (Wash. DC)*. 215:1243-1245.
54. Selkoe, D. J., C. R. Abraham, M. B. Podlinsky, and L. K. Duffy. 1986. Isolation of low-molecular-weight proteins from amyloid plaque fibers in Alzheimer's disease. *J. Neurochem.* 46:1820-1834.
55. Shapira, R., G. E. Austin, and S. S. Mirra. 1988. Neuritic plaque amyloid in Alzheimer's disease is highly racemized. *J. Neurochem.* 50:69-74.
56. Shaw, G., and V. Chau. 1988. Ubiquitin and microtubule associated protein tau immunoreactivity each define distinct structures with different distributions and solubility properties in Alzheimer brain. *Proc. Natl. Acad. Sci. USA* 85:2854-2858.
57. St. George-Hyslop, P. H., R. E. Tanzi, R. J. Polinsky, J. L. Haines, L. Nee, P. C. Watkins, R. H. Myers, R. G. Feldman, D. Pollen, D. Drachman, J. Growdon, A. Bruni, J. F. Foncin, D. Salmon, P. Frommelt, L. Amaducci, S. Sorbi, S. Piacentini, G. D. Stewart, W. J. Hobbs, P. M. Conneally, and J. F. Gusella. 1987. The genetic defect causing familial Alzheimer's disease maps on chromosome 21. *Science (Wash. DC)*. 235:885-890.
58. Tanzi, R. E., J. F. Gusella, P. C. Watkins, G. A. P. Bruns, P. St. George-Hyslop, M. L. Van Keuren, D. Patterson, S. Pagan, D. M. Kurnit, and R. L. Neve. 1987. Amyloid  $\beta$  protein gene: cDNA, mRNA distribution, and genetic linkage near the Alzheimer locus. *Science (Wash. DC)*. 235:880-884.
59. Tanzi, R. E., P. H. St. George-Hyslop, J. L. Haines, R. J. Polinsky, L. Nee, J. F. Foncin, R. L. Neve, A. I. McClatchey, P. M. Conneally, and J. F. Gusella. 1987. The genetic defect in familial Alzheimer's disease is not tightly linked to the amyloid  $\beta$  protein gene. *Nature (Lond.)*. 329:156-157.
60. Tanzi, R. E., A. I. McClatchey, E. D. Lamperti, L. Villa-Komaroff, J. F. Gusella, and R. L. Neve. 1988. Protease inhibitor domain encoded by an amyloid protein precursor mRNA associated with Alzheimer's disease. *Nature (Lond.)*. 331:528-530.
61. Terry, R. D., and R. Katzman. 1983. Senile dementia of the Alzheimer type. *Ann. Neurol.* 14:497-506.
62. Terry, R. D., and H. Wisniewski. 1970. The ultrastructure of the neurofibrillary tangle and the senile plaque. *Ciba Symp.* 145-165.
63. Terry, R. D., N. K. Gonatas, and M. Weiss. 1964. Ultrastructural studies in Alzheimer's presenile dementia. *Am. J. Pathol.* 44:269-297.
64. Tomlinson, B. E. 1979. The ageing brain. In *Recent Advances in Neuropathology*. W. T. Smith and J. B. Cavanagh, editors. Churchill Livingstone Inc. New York. 129-159.
65. Tomlinson, B. E., and J. A. N. Corsellis. 1984. Ageing and the dementias. In *Greenfields' neuropathology*. J. Hume-Adams, J. A. N. Corsellis, and L. W. Duchem. John Wiley & Sons Inc., New York. 951-1025.
66. Van Broeckhoven, C., A. M. Genthe, A. Vandenberghe, B. Horsthemke, H. Backhovens, P. Raeymaekers, W. Van Hul, A. Wehnert, J. Gheuens, P. Cras, M. Bruyland, J. J. Martin, M. Salbaum, G. Multhaup, C. L. Masters, K. Beyreuther, H. M. D. Gurling, M. J. Mullan, H. Holland, A. Barton, N. Irving, R. Williamson, S. J. Richards, and J. A. Hardy. 1987. Failure of familial Alzheimer's disease to segregate with the A4-amyloid gene in several European families. *Nature (Lond.)*. 329:153-155.
67. Vaughan, D. W., and A. Peters. 1981. The structure of neuritic plaques in cerebral cortex of aged rats. *J. Neuropathol. & Exp. Neurol.* 40:472-482.
68. Wells, C. E. 1985. Organic syndromes: dementia. In *Comprehensive Textbook of Psychiatry*. H. I. Kaplan and B. J. Sadock, editors. Williams and Wilkins, Baltimore. 851-869.
69. Wisniewski, H. M., and R. D. Terry. 1973. Re-examination of the pathogenesis of the senile plaque. *Progr. Neuropathol.* 2:1-26.
70. Wisniewski, H. M., B. Ghetti, and R. D. Terry. 1973. Neuritic (senile) plaques and filamentous changes in aged rhesus monkeys. *J. Neuropathol. & Exp. Neurol.* 32:566-584.
71. Wisniewski, H. M., A. W. Vorbrodt, R. C. Moretz, A. S. Lossinsky, and I. Grundke-Iqbal. 1982. Pathogenesis of neuritic (senile) and amyloid plaque formation. *Exp. Brain Res. Suppl.* 5:3-9.
72. Wood, J. G., S. S. Mirra, N. J. Pollock, and L. I. Binder. 1986. Neurofibrillary tangles of Alzheimer's disease share antigenic determinants with the axonal microtubule-associated protein tau (T). *Proc. Natl. Acad. Sci. USA*. 83:4040-4043.
73. Zain, S. B., M. Salim, W. G. Chou, E. M. Sajdel-Sulkowska, R. E. Majocha, and C. A. Marotta. 1988. Molecular cloning of amyloid cDNA derived from mRNA of the Alzheimer's disease brain: coding and non-coding regions of the fetal precursor mRNA are expressed in the cortex. *Proc. Natl. Acad. Sci. USA*. 85:929-933.